

SINGLE CRYSTAL ZnO NANOWIRE LUMINESCENCE SHIFTING BY NANOSTRUCTURED ZnO LAYERS

A.MARCU^a, I.ENCULESCU^d, S.VIZIREANU^{a,e}, R.BIRJEGA^a,
C.POROSNICU^{a*}

^aNational Institute for Laser, Plasma and Radiation Physics, Atomistilor 409,
P.O.Box MG 36, Bucharest-Magurele, Romania

^bNational Institute for Material Physics, Atomistilor 105bis, P.O.Box MG 47,
Bucharest-Magurele, Romania

^cPetroleum-Gas University of Ploiesti, Bucuresti 39, P.O.BOX 52, 100680-
Ploiesti, Romania

Single crystal ZnO nanowires grown by pulsed laser deposition (PLD) and vapour-liquid-solid (VLS) technique respectively, were in-situ and ex-situ covered with additional ZnO shell layers. Luminescence investigation revealed significant luminescence spectra shift from UV to blue emission band of the obtained structures while changing the deposited shell layer film thickness. But with no monotone variation with the deposited film thicknesses. While the luminescence changes are generally considered as being determined by the ratio between core emission lines intensity and shell 'defects' lines intensity, the strongest changes in the photoluminescence spectra were obtained in our experiments for the nanometer order shell layer thicknesses. The comparison between luminescence results and luminescence studies on 50 nm ZnO nanoparticles clusterization, together with HRTEM investigations of the ZnO shell layer suggest that the nanoparticle-nanowire interface, respectively the coupling between the ZnO single crystal core and ZnO nanostructured shell layer, might play a significant role in the luminescence spectra changes.

(Received January 7, 2013; Accepted March 26, 2013)

Keywords: ZnO luminescence, core-shell nanostructures, special PLD, PLD/PR,
ZnO nucleation

1. Introduction

Zinc oxide is known as a wide band-gap semiconductor material with a large exciton binding energy (60 meV). ZnO nanomaterials are promising candidates for nanoelectronics and photonics and an intense interest has been paid to its optical and electronic properties [1-12]. As the dimension reduces to the nanometer range, the properties change significantly from the bulk material [13-15] generating novel physical features for applications [17, 18]. Particularly the luminescence properties are size related features based on quantum confinement effect and respectively surface states, and have drawn lots of investigations [18-21]. Nanorods arrays devices [22] and even single wire devices became technically possible [23-26] and tuning the optical properties of nanowires became an issue of the present research.

Starting from single crystal ZnO nanowires grown by pulsed laser deposition (PLD) and vapor-liquid-solid (VLS) technique and by using PLD technique for depositing in-situ and ex-situ additional ZnO shell layers over the ZnO nanowires, here, we investigate the changes from the photoluminescence spectra of the resulting ZnO nanostructure

*Corresponding author: c.porosnicu@yahoo.com

2. Materials and methods

We have grown zinc oxide nanowires using a special PLD system with plasma reflection (PLD/PR) and respectively VLS growing technique. In figure 1 a generic scheme of the experimental setup for this system is given, while more details on the oxide nanowire fabrication using PLD/VLS and some plume filtering techniques using such a fabrication method were given elsewhere [27-30]. In this experiment we used a picosecond LUMERA Fast laser reaching a 500 kHz repetition rate and about 1.5 W beam power at 355 nm wavelength. Ablation target was a sintered target made from commercially available ZnO nanopowder with 50 nm particle diameter and gold droplets were used as liquid catalyst for the VLS process. The substrate was [1120] alumina. Ambient pressure was 1 Pa (oxygen) and substrate temperature around 800^o C. For the deposition of the ZnO shell layer, the experimental system was the same and deposition condition similar, except the temperature which was varying between nanowire growing conditions and room temperature. The shell layer was made in some cases 'in-situ' – meaning depositing the shell layer just after the fabrication process, without moving the sample or taking the sample out of the chamber – and in some cases 'ex-situ' – respectively by removing the sample from the chamber for measurements and repositioning the sample for the next shell layer deposition step. The samples were investigated using X-ray diffraction (XRD) (Panalytical X'Pert MRD with CuK α (λ = 0.15918 nm)), scanning electron microscopy (FEI Quanta, E=50 keV), transmission electron microscopy (Jeol 2010F operated at 200kV with a point to point resolution of 0.19 nm) and photoluminescence (Edinburgh Instruments FS-920D) using a laser excitation with 350 nm wavelength.

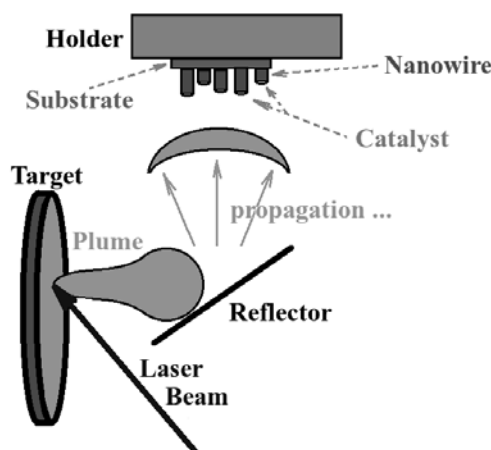


Fig. 1 Experimental setup

3. Results

ZnO nanowires grown with our PLD/VLS experimental system (Fig. 2a) were used as the core for the ZnO core-shell investigated structures. An additional ZnO layer was deposited over the VLS grown nanowires. Shell layer deposition was done at room temperature (\sim 25^o C). At the room temperature the gold catalyst was solidified and the particle's diffusion over substrate surface was reduced, so the growing mechanism was no longer VLS but thin film growing. The resulting structure is a core ZnO nanowire covered with a ZnO shell layer. From the morphology point of view, the only observable change for a 15 minutes shell layer deposition is a slight increase of the wire diameter in the order of a few tens on nanometers.

A second ZnO core-shell structure was fabricated starting from the same ZnO nanowires, but with the additional layer ZnO layer deposited at variable temperature using an in-situ process. Thus, the deposition time was extended with 15 minutes while keeping all parameters constant, excepting the substrate temperature which was gradually decreasing down to below 200^o C, in this interval. While decreasing the temperature, the dominant growing process gradually changes from nanowire growing process to the thin film growing process and wires were covered in-situ with an additional ZnO shell layer. Below 450^o C and using gold catalyst we can consider that gold

at catalyst solidify and the VLS nanowire growing process actually stops [31-33] in its competition with the thin film growing process. Still the resulting morphology looks considerably similar to the previous core-shell structure. The wire diameter increase is also in the range of few tens of nanometers, as seen in Fig. 2b.

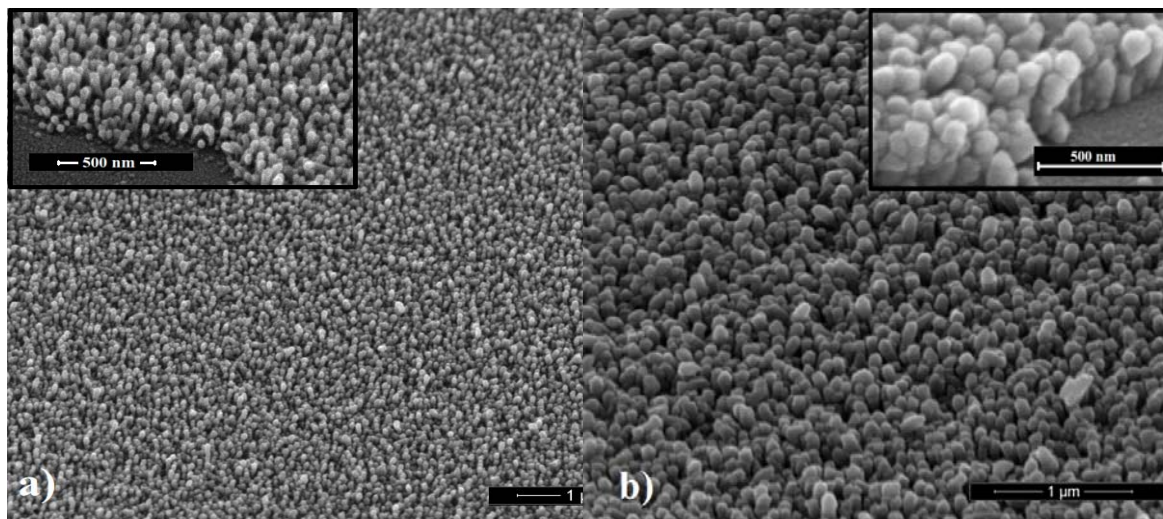


Fig. 2 SEM images of a) uncovered ZnO wires, b) core-shell ZnO structures and XRD pattern from core-shell ZnO structures

Our X-ray investigations of the uncovered ZnO nanowires and respectively core-shell structures could not distinguish significant differences between the diffraction patterns of the three samples; therefore, we present in Fig. 2C only the diffraction pattern for the room temperature shell layer deposited structure. All the XRD spectra exhibited a predominant [0001] oriented structure with no significant changes determined by the presence of the shell layer, at least from the long range order crystalline structure approach. The fact that the shell layer does not significantly change the [14-15] peak (Fig. 2c), (usually assigned to some droplets from the laser ablation process but also with the miss oriented ZnO crystals) suggests that there are no major variations in the volume ratio of [0001] grown structures and other orientations. Thus, we can assume that the deposited shell layers are predominantly having a [0001] grown orientation following the core structure or an amorphous structure.

TEM investigation on the ZnO nanowires has shown a single “zincite” structure, a wurtzite with hexagonal symmetry, which is typical for ZnO. The growing orientation is [0001] and the facing planes are (01-10) family with a relatively smooth surface (Fig. 3a). Particular attention was given to the room temperature deposited shell layer, which was expected to cause the most important changes of the shell layer (from the VLS grown core structure). HR-TEM investigations of the shell layer have shown an amorphous structure in most of the observed areas (Fig. 3b). However, there are also areas where a polycrystalline structure has been revealed. As can be seen in the power spectrum (FFT) from Fig. 3c inset, there is a clear ring referred to (0002) planes of zincite (2.61 nm) so we can say that the shell layer is made of a polycrystalline zincite structure in this area. ZnO nanoparticles are also visible in the shell layer of the covered nanowires (Fig. 3d). The nanoparticles seem to have a similar structure with the core and they are spread over the core surface area. In spite of the fact that these nanoparticles are embedded in polycrystalline or amorphous layers of ZnO, the mismatch between their structure and the core's one seems to be, predominantly, a low one.

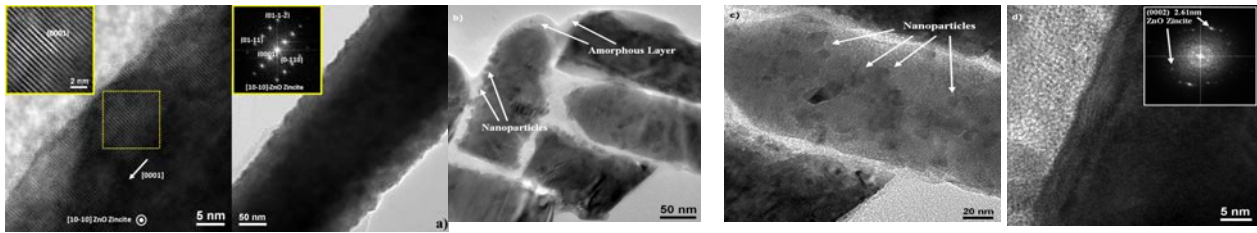


Fig. 3. HR-TEM images of: a) uncovered ZnO wires, b) ZnO core-shell structures, c) ZnO particles embedded into amorphous shell layer and d) diffraction pattern of polycrystalline 'zincite' shell layer

The HR-TEM investigations have shown that the nanoparticles have also a 'zincite' structure, same as the nanowires (Fig. 4 lower inset). Even if there might sometimes be slight differences in crystal axis orientation between core and shell structures (in the presented case Fig. 4 upper inset is 4.7°) there is predominantly a "good bound" between these structures. We should mention the fact that this "bound" should actually be formed from the early stages of the nanoparticle growing over the core surface which for a film growing process should correspond to the initial 'island grow' stage.

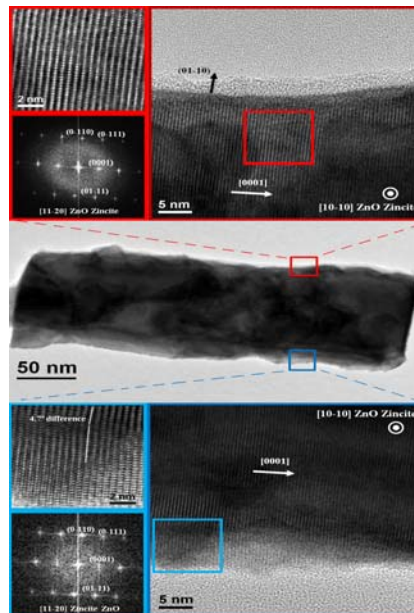


Fig. 4. HR-TEM images of ZnO core-shell structure with a 4.7° mismatch between the nanoparticle and core crystal structure orientations in the lower inset and a perfect match between core and shell structures in the upper inset

In terms of luminescence spectra the changes induced by the additional ZnO shell layer are rather significant. While exciting the ZnO structures with a 350 nm laser beam, the luminescence main peak changes from about 375 nm corresponding to the uncovered nanowires to 420-433 nm for the covered structures (Fig. 5). It is also interesting to mention that the luminescence response of room temperature covered structure is still in the same blue band and rather similar with the variable temperature shell layer structure spectra, excepting that the luminescence band tends to be slightly broader.

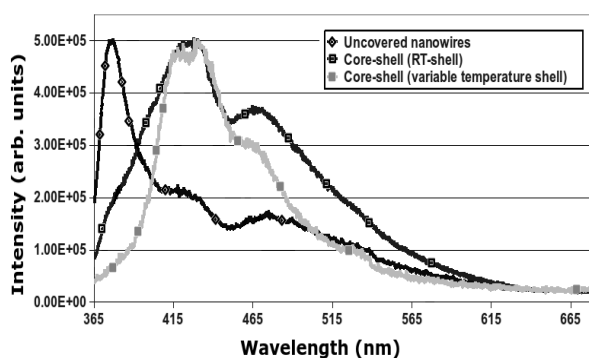


Fig. 5 Photoluminescence spectra of covered and uncovered ZnO nanowires

In order to understand the transition between the core and core-shell luminescence spectra, we analyze the PL of the ZnO nanowire structures while we deposit over the ZnO core, 'ex-situ', additional layers of ZnO. The deposition time of the shell layers was gradually increased from 1 to 8 minutes while recording the luminescence spectra after each step. The measurements presented in Figure 6a were made on the same sample consequently covered with thicker and thicker shell layers. From the luminescence curves (normalized to the maximal intensities), we see that while deposited layer becomes thicker, the blue band relative intensity peaks gradually increase and the core structures UV peak decreases. There is no wavelength tuning into this process. There is only a decrease of the 375 nm luminescence peak and a blue emission band (420 - 433 nm) increase.

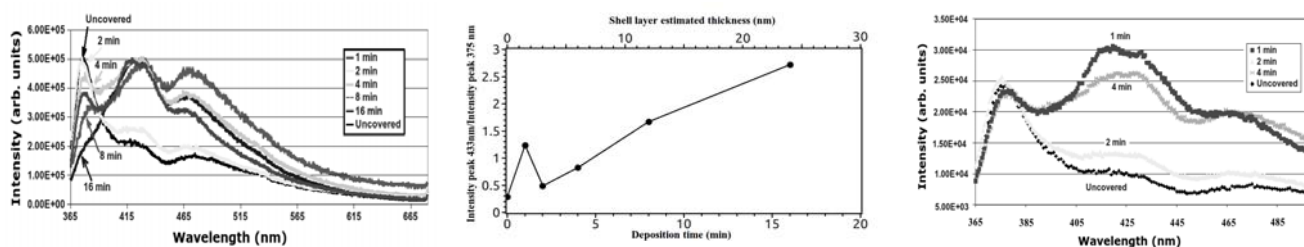


Fig. 6 Thickness dependence of the ZnO core-shell structure's photoluminescence: a) normalized spectra (to maximal value) for different shell layer thicknesses, b) ratio between intensities of blue and UV emissions and c) non-normalized spectra for thin additional ZnO layers

A plot of the ratio between 433 nm and 375 nm peak amplitude is showing a quasi-linear variation with the deposition time, respectively the shell layer (average) thickness (Fig. 6b). Still, there is one layer thickness which does not fit to the main trend. The apart spectrum corresponds to a very thin shell layer. The thickness of the shell layer is estimated for this sample below 1 nm. By further comparing the non-normalized PL spectra lines for no-shell, 1, 2 and 4 minute deposited shell layer (Fig. 6c), we could notice that there is actually no significant change of the 375 nm peak corresponding to the luminescence of the ZnO nanowires in this early stages of the shell formation but rather a non-monotone variation of the 420 nm and 433 nm emission peaks intensities. The decrease of the nanowire UV emission (375 nm) becomes evident for later stages, corresponding to thicker shell layers (> 5 nm).

4. Discussions

The modification of ZnO luminescence spectra is generally considered as being related to the changes in the ZnO structure [34,35]. In our case, the changes in the luminescence spectra should be related to the additional ZnO deposited layer and respectively shell layer 'defects'.

During the additional ZnO deposition process the decrease of the temperature affects not only the VLS growing process but the crystalline structure and morphology of the additional layers as well. With the decrease of temperature, ZnO growing structure should also change from good crystallinity with fewer defects at higher temperatures [36-38] to polycrystalline or even amorphous structure for lower temperatures [39-41].

The UV peak (375 nm) is explained in literature with the ZnO structure's two electron [42,43] or free exciton [44,45] transitions and more recently with the stacking faults [21, 46] and physically associated with the core nanowires. Lower energy peaks (420, 433 and 467 nm) are partially assigned [47-49] still under discussion but assumed to belong to defects in the crystal structures. In our case should be associated with the presence of the shell layer. However, the 433 nm luminescence peak, which is actually the strongest of the covered structure spectra, could also be obtained from the 50 nm crystalline ZnO nanoparticles (also used for the target sinterization). ZnO nanoparticles were simply sonicated in water for 5 minutes (1mg/10 cc) and we obtained a similar dominant luminescence peak at 433 nm. But, if the solution is centrifuged in order to deposit the 'dense' clusters, the blue emission is no longer the dominant peak and the resulted emission nears significantly to the ZnO core emission band (Fig. 7a). Furthermore, the centrifuged sample luminescence spectra are independent on centrifugation acceleration (Fig. 7b). Since, on one side, the centrifugation speed proved to control the cluster size [50] but, on the other side, has no relevance for this spectrum, the 433 nm peak would probably not be related with the nanoparticle size (since the nanoparticles from the solution should roughly have same size of about 50 nm), but rather associated with the presence of very big and 'dense' clusters. Thus, the nanoparticle's clusterization should probably be somehow associated with the main blue luminescence peak line from 433 nm.

The obtained luminescence results have shown that while the intensity of the core associated peaks tends to gradually decrease with the shell layer thickness, the shell layer associated peaks is rather having a discontinuous variation, particularly at the incipient stages of the shell layer formation.

One possible interpretation of the non-uniform variation of the blue emission could be related to the shell nanoparticles growing in the early stages of the layer formation. By taking into consideration the non uniform plume penetration between wires because of the substrate morphology (Fig. 1), the cluster presence in laser plume and the low deposition temperature ($\sim 25^{\circ}\text{C}$) which drastically reduce the particle diffusion over the sample surface, we have to assume an "island grow" (non-continuous) morphology of the shell layer covered at low temperatures. Some previous studies proved absorption spectra movement toward UV with the nanoparticle size decreasing [7], so the structures formed on the core surface could play an important role in changing the luminescence spectra of the structure. Thus, the initial small nanoparticles should have a more efficient absorption and respectively emission while at later stages, the layer thickness would be the controlling factor of the UV absorption. This might be in agreement with the 433nm/375nm intensity variation/oscillations at early stage of the shell layer formation. However, the changes in the shell nanoparticle size are not observable in the emission spectra so the particle's average size is not changing significantly during shell layer thickness growing process or the change in their average size is not an issue for the emission process which make this assumption as 'questionable'.

Another possibility is to speculate that if the bound between ZnO nanoparticles is indeed associated with the blue (433 nm) peak in the water solution luminescence response, the good particle-core bound might also be responsible on the 433 nm emission from the ZnO nanostructures. In this case, this emission line should be characteristic to the nanoparticle-nanowire / nanoparticle-nanoparticle interface (bound) rather than the core or the shell independently. In this case, the diminishing of the UV peak would be related only with the amorphous/polycrystalline layer absorption, which is in no direct relation with the presence of the emitting nanoparticles over the core surface, while the emitting lines should correspond to the deposited/grown particles but also to the nanoparticle-nanowire interface (bounding) area. This could explain why the blue line emission is not directly linked with the film thickness (particularly the 433 nm peak) while the decrease of the UV emission is only depending on the shell layer thickness increase through the absorption processes.

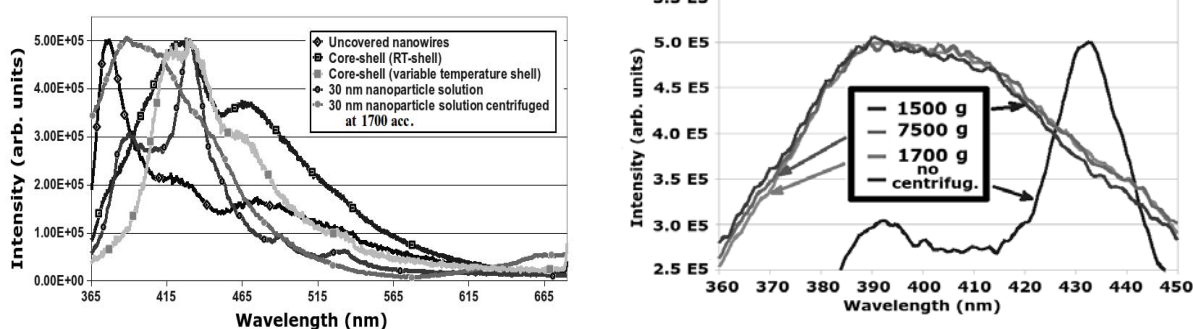


Fig. 7 Luminescence spectra from water solution of 50 nm ZnO nanoparticles a) as produces and centrifuged for 30 minutes with accelerations of 1700 g, and b) for several centrifugation accelerations: 1700 g, 7500 g and 15000 g

5. Conclusions

In conclusion, using PLD/VLS growing technique, the photoluminescence of the core-shell ZnO nanostructures could be significantly shifted from UV to blue 420-433 nm emission band, only by using ZnO shell layer with thicknesses within nanometer range. The change in the luminescence spectra is understood as a balance between core emission and shell nanoparticle emission. While the core emission would decrease with the increase of the thickness of the polycrystalline/amorphous shell layer due to the absorption processes, the blue emission would depend on the presence and possible good bond between the ZnO nanoparticles and the single crystal ZnO core structure. For a ZnO shell layer with the thickness below 1 nm, both UV and blue band peaks could be obtained, enlarging the emission spectra and potentially enhancing the structure global photoluminescence efficiency.

Acknowledgments

This work was partially supported by the PosDru/89/1.5/S/60746. Vizireanu S. acknowledges funding from the European Social Fund through POSDRU/89/1.5/S/54785 project: "Postdoctoral Program for Advanced Research in the field of nanomaterials" and Porosnicu C. for CNCS – UEFISCDI grant, PN-II-IDPCE- 2011-3-0522. The authors would like to thank to R.ZAMANI (ICMAB-CSIC, IREC), J.R.MORANTE (IREC, Universitat de Barcelona), J.ARBOL (ICMAB-CSIC, ICREA) and TEM facilities in Serveis Científicotècnics from Universitat de Barcelona.

References

- [1] M.H. Huang, S. Mao, H. Feick, H.Q. Yan, Y.Y. Wu, H. Kind, E. Weber, R. Russo, P.D. Yang, *Science* **292**, 1987(2001).
- [2] X.W.Sun, H.S.Kwok, *J.Appl. Phys.* **86**, 408 (1999).
- [3] S.J. Jiao, Z.Z. Zhang, Y.M. Lu, D.Z. Shen, B. Yao, J.Y. Zhang, B.H. Li, D.X. Zhao, X.W. Fan, Z.K. Tang, *Appl. Phys. Lett.* **88**, 031911 (2006).
- [4] A.Marcu, T.Yanagida, K.Nagashima, H.Tanaka and T.Kawai, *J. Appl. Phys.* **102**, 023713 (2007)
- [5] M. Caglar, S. Ilican, Y. Caglar, F. Yakuphanoglu, *Appl. Srf. Sci.* **255**, 4491 (2009).

- [6] E. Alarcon-Llado, S. Estrade, J.D. Prades, F. Hernandez-Ramírez, J. Arbiol, F. Peiró, J. Ibáñez, L. Artús, J.R. Morante, *CrystEngComm*, **13**, 656 (2011)
- [7] J. Fan, A. Shavel, R. Zamani, C. Fábrega, J. Rousset, S. Haller, F. Guell, A. Carrete, T. Andreu, J. Arbiol, J.R. Morante, A. Cabot, *Acta Materialia* **59**, 6790 (2011).
- [8] M. I. B. Utama, F. J. Belarre, C. Magen, B. Peng, J. Arbiol, Q. Xiong, *Nano Lett.* **12**, 2146 (2012).
- [9] J.D. Fan, C. Fábrega, R. Zamani, A. Shavel, F. Güell, A. Carrete, T. Andreu, A.M. López, J.R. Morante, J. Arbiol, A. Cabot, *Journal of Alloys and Compounds*, 555, 213, 2013
- [10] J.D. Fan, R. Zamani, C. Fábrega, A. Shavel, C. Flox, M. Ibáñez, T. Andreu, A.M. López, J. Arbiol, J.R. Morante, A. Cabot, *Journal of Physics D: Applied Physics*, 45, 415301, 2012
- [11] M. de la Mata, C. Magen, J. Gazquez, M. I. B. Utama, M. Heiss, S. Lopatin, F. Furtmayr, C. J. Fernandez-Rojas, B. Peng, J. R. Morante, R. Rurali, M. Eickhoff, A. Fontcuberta I Morral, Q. Xiong, J. Arbiol, *Nano Lett.* **12**, 2579 (2012).
- [12] J. Arbiol, C. Magen, P. Becker, G. Jacopin, A. Chernikov, S. Schäfer, F. Furtmayr, M. Tchernycheva, L. Rigutti, J. Teubert, S. Chatterjee, J. R. Morante, M. Eickhoff *Nanoscale*, **4**, 7517-7524 (2012)
- [13] X.Y. Kong, Y. Ding, R. Yang, Z.L. Wang, *Science* **303**, 1348 (2004)
- [14] D. Segets, J. Gradl, R. K. Taylor, V. Vassilev and W. Peuker, *ACS Nano*, **3**, 1703 (2009)
- [15] S. Nakamura, M. Senoh, N. Iwasa, T. Yamada, T. Matsushita, Y. Sugimoto, H. Kiyoku, *Appl. Phys. Lett.* **69**, 1568 (1996)
- [16] O. L. Stroyuk, V. M. Dzhagan, V. V. Shvalagin and S. Ya. Kuchmiy, *J. Phys. Chem. C* **114** 220 (2010).
- [17] Y. Kayanuma, *Phys. Rev. B* **38**, 9797 (1988)
- [18] L. Zhang, L. Yin, C. Wang, N. Lun, Y. Qi and D. Xiang, *J. Phys. Chem. C*, **114**, 9651 (2010).
- [19] I. Shalish, H. Temhin, V. Narayanamurti, *Phys. Rev. B* **69**, 245401 (2004).
- [20] X.Wang, F.Zhao, P.Xie, S.Liang, S.Deng and N.Xu, *Optics Communications* **276**, 180 (2007).
- [21] H. He, Q. Yang, C. Liu, L. Sun, and Zhizhen Ye, *J. Phys. Chem. C*, **115**, 58 (2011).
- [22] A. Qurashi, M.F. Hossain, M. Faiz, N. Tabet, Mir Wakas Alam, N. Koteeswara Reddy, *J. Alloys and Compounds*. **503**, L40 (2010).
- [23] Y.Q. Bie, Z.M. Liao, P.W. W., Y.B. Zhou, X.B. Han, Y. Ye, Q. Zhao, X.S. Wu, L. Dai, J. Xu, L.W. Sang, J.J. Deng, K. Laurent, Y. Leprince-Wang and D.P. Yu, *Adv. Mater.* **22**, 4284 (2010).
- [24] L. X. Mu, W. S. Shi, T. P. Zhang, H. Y. Zhang, Y. Wang, G. W. She, Y. H. Gao, P. F. Wang, J. C. Chang, and S. T. Lee, *Appl. Phys. Lett.* **98**, 163101 (2011)
- [25] K. Kim, H.g Kang, H. Kim, J. S. Lee, S. Kim, W. Kang and G.T. Kim, *Appl. Phys. A*, **94**, 253 (2009).
- [26] F. Hernández-Ramírez, A. Tarancón, O. Casals, J. Arbiol, A. Romano-Rodríguez, J.R. Morante, *Sensors and Actuators, B: Chemical*, **121**, 3 (2007).
- [27] A. Marcu, L. Trupina, R.Zamani, J.Arbiol, C. Grigoriu and J. R. Morante, *Thin. Solid Films* **520**, 4626 (2012).
- [28] A.Marcu, T.Yanagida, K.Nagashima, H.Tanaka and T.Kawai, *J. of Appl. Phys.*, **102**, 016102 (2007).
- [29] A.Marcu, C. Grigoriu, C.P.Lungu, T.Yanagida and T.Kawai in *Phys. E* **44**, 1071 (2012).
- [30] A.Marcu, M.Goyat, T.Yanagida and T.Kawai, *J. of Opt. and Adv. Mat.* **11**, 421 (2009).
- [31] S. Kodambaka, J. Tersoff, M. C. Reuter and F. M. Ross, *Science* **316**, 729 (2007).
- [32] Y.T. Yin, Y.-Z. Chen, C.-H. Chen and L.Y. Chen, *J. Chin. Chem. Soc.*, **58**, 1 (2011).
- [33] Liu, H. S.; Ishida, K.; Jin, Z. P.; Du, Y. *Intermetallics* **11**, 987 (2003).
- [34] D. Dou, H. L. Mosbacher, G. Cantwell, J. Zhang, J. J. Song, L. J. Brillson, *Appl. Phys. Lett.* **94**, 042111 (2009).
- [35] Yi-Hao Pai and Gong-Ru Lin, *J. Electrochem. Soc.*, **158**, E88 (2011).
- [36] K. Nagashima, T. Yanagida, H. Tanaka, and T. Kawai, *Appl. Phys. Lett.* **90**, 233103 (2007).
- [37] S. A. Dayeh, E. T. Yu, and D.Wang, *Nanoletters* **7**, 2486 (2007).

- [38] H. W. Kim, M. A. Kebede, H. S. Kim, B. Srinivasa, D. Y. Kim, J. Y. Park, S. S. Kim
Current Appl. Phys. **10**, 52 (2010).
- [39] S. Singh, **R.S. Srinivasa and S.S. Major, Thin Solid Films 515, 8718 (2007).**
- [40] S. Aksoy, Y. Caglar, S. Ilican and M. Caglar, Adv. in Cntrl., Chem. Eng., Civil Eng. and
Mech. Eng. (2010) pp 227, ISBN: 978-960-474-251-6
- [41] J.-H. Kim and E. K. Kim, Phys. Stat. Sol. (b) **244**, 1500 (2007).
- [42] S.A. Studenikin, M.Cocivera, W.Kellner and H.Pasher, J. Luminescence **91**, 233 (2000).
- [43] D.C.Reynolds and T.C. Collins, Phys. Rev. **185**, 1099 (1969).
- [44] A. Teke, Ü. Özgür, S. Doğan, X. Gu, and H. Morkoç, Phys. Rev. B **70**, 195207 (2004).
- [45] C.Klingshirn, J.Fallert, O.Gogolin, M.Wissinger, R.Hauschild, M.Hauser, H.Kalt and
H.Zhou, J Luminescence **128**, 792 (2008).
- [46] M.Shirra, R.Schneider, A.Reiser, G.M.Prinz, M.Feneberg, J.Biskupek, U.Kaiser, C.E.Krill,
K.Thonke and R.Sauer, Phys. Rev. B **77**, 125215 (2008).
- [47] S.K.Mishra, R.K.Srivastava, S.G.Prakash, R.S.Yadav and A.C.Panday, Opt.-Electr. Rev.
18, 467 (2010).
- [48] Z. Fang, Y. Wang, D. Xu, Y. Tan and X. Liu, Opt. Mat. **26**, 239 (2004).
- [49] L.H. Zhao and S.Q. Sun, CrystEngComm, **13**, 1864 (2011),
DOI. 10.1039 / C0CE00548G
- [50] A.Marcu, C.Sima, C.Grigoriu, I.Enculescu and B.Iliescu, J. Optoelectron. Adv. Mater.
10, 3131 (2008).